

Metabolites from the marine-facultative *Aspergillus* sp. MEXU 27854 and *Gymnoascus hyalinosporus* MEXU 29901 from Caleta Bay, Mexico

By: Manuel A. Aparicio-Cuevas, María del Carmen González, [Huzefa A. Raja](#), Isabel Rivero-Cruz, Steven J. Kurina, Joanna E. Burdette, [Nicholas H. Oberlies](#), and [Mario Figueroa](#)

Aparicio-Cuevas, M.A., González, M.D.C., Raja, H., Rivero-Cruz, I., Kurina, S.J., Burdette, J.E., Oberlies, N.H., & Figueroa, M. (2019). Metabolites from the marine-facultative *Aspergillus* sp. MEXU 27854 and *Gymnoascus hyalinosporus* MEXU 29901 from Caleta Bay, Mexico. *Tetrahedron Letters* 60(25), 1649-1652.

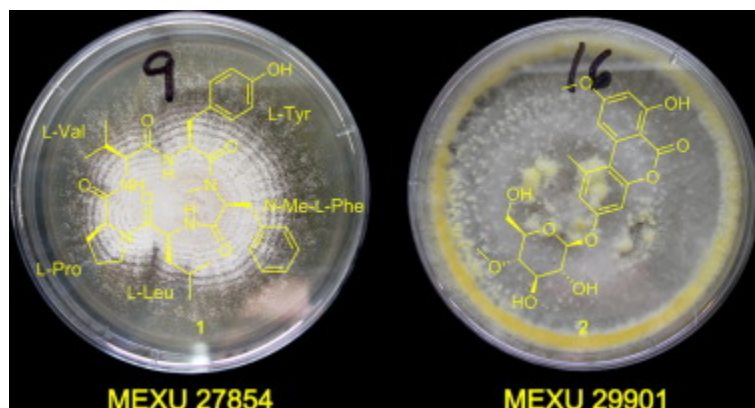
Made available courtesy of Elsevier: <https://doi.org/10.1016/j.tetlet.2019.05.037>



© 2019 Elsevier Ltd. This work is licensed under a [Creative Commons Attribution-NonCommercial-NoDerivatives 4.0 International License](#).

Abstract:

During our ongoing research on fungal strains from unexplored sources, the reinvestigation of the CHCl₃–MeOH extract of the marine-facultative *Aspergillus* sp. MEXU 27854 yielded a new *N*-methyl cyclic pentapeptide (**1**) along with known butyrolactone II and PF1233 A. In addition, from the marine-facultative *Gymnoascus hyalinosporus* MEXU 29901, a new alternariol glucoside, 10-*O*-[β -d-(4-methoxyl-glucopyranosyl)]-4-*O*-methylalternariol (**2**) and known alternariol 4-*O*-methyl ether, alternariol and beauvericin, were isolated. The structures of **1** and **2** were established by detailed spectroscopic data, and their absolute configuration was ascertained by Marfey's analysis and HRESIMS-MS/MS data for **1**, and by chemical degradation and optical rotation analysis for **2**.



Keywords: Fungi | Unexplored | Ascomycetes | Metabolites

Article:

Fungi are considered one of the most diverse group of organisms with over 120,000 currently recognized species and an estimated of 2.2 to 3.8 million worldwide [1]. Mycodiversity of

Mexico has been poorly studied, and some authors have proposed the existence of around 200,000 fungal species, but less than 10,000 remain taxonomically described [2], and even fewer investigated for their secondary metabolites chemistry [3]. Thus, fungal species isolated from unexplored sources in Mexico represent an important source of new chemical diversity and bioactive compounds.

During our ongoing research on fungal strains from different regions of Mexico, a sample of sand from the intertidal zone of Caleta Bay in Acapulco, Guerrero, Mexico, was collected. From this, several fungal strains were isolated, and the chemical study of a marine-facultative *Aspergillus* sp. MEXU 27854 yielded a series of new dioxomorpholines [4]. In this work, we describe the reinvestigation of this strain and include the characterization of a new *N*-methyl cyclic pentapeptide, caletasin (**1**), the known butyrolactone II and the dioxomorpholine PF1233 A. Furthermore, from another marine-facultative fungus isolated from the same sample of sand, *Gymnoascus hyalinusporus* MEXU 29901, a new alternariol glucoside (**2**) and the known alternariol 4-*O*-methyl ether, alternariol, and beauvericin were obtained. It is interesting that the genus *Gymnoascus* is greatly understudied despite its ubiquitous distribution. *Gymnoascus dankaliensis*, *G. aurantiaca*, *G. reessii*, and *G. cetosus* are the only species studied for their secondary metabolites production [5], [6], [7], [8], [9], [10], [11], [12], [13], [14], [15]. As such, this is the first chemical study of *G. hyalinusporus*.

Solid-phase cultures of *Aspergillus* sp. MEXU 27854 and *G. hyalinusporus* MEXU 29,901 (Figs. S1 and S2) were extracted with CHCl₃–MeOH (1:1), and the resulting dry extracts were partitioned between *n*-hexane and CH₃CN–MeOH (1:1). Extensive chromatographic fractionation and purification of the defatted extracts using preparative RP-HPLC resulted in the isolation and purification of new compounds **1** and **2** along with several known metabolites (Fig. 1), butyrolactone II, PF 1233A, alternariol 4-*O*-methyl ether, alternariol, and beauvericin, whose identity was corroborated by comparison with reported data (Table S1 and Figs. S3–S8) [16], [17], [18], [19], [20].

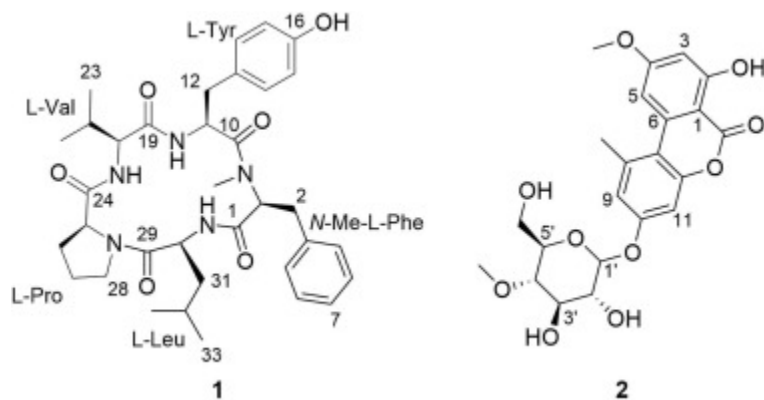


Figure 1. Structures of compounds **1** and **2**.

Compound **1** [21] was obtained as an orange powder. Its molecular formula was deduced as C₃₅H₄₇N₅O₆ based on the molecular ion peak at *m/z* 634.3596 [M + H]⁺ in the HRESIMS (Fig. S8), establishing an index of hydrogen deficiency (IHD) of 15. A detailed analysis of the 1D and 2D NMR spectral data (Table 1 and Figs. S9–S12) revealed that this compound has a peptide structure, with a profile similar to that of cotteslosin B [22]. Some key differences between **1** and

cotteslosin B are the presence of one, instead of two, phenolic hydroxy group at δ_{H} 9.02 (1H, s, 16-OH); a disubstituted ring system represented by a double doublets at δ_{H} 6.54 (2H, d, $J = 8.4$ Hz, H-15 and H-17) and 6.65 (2H, d, $J = 8.4$ Hz, H-14 and H-18) from the aromatic protons of a Tyr residue (Fig. S13); and 10 protons of a Leu residue at δ_{H} 4.62 (1H, m, H-30), 1.79 (1H, m, H_{2a}-31), 1.29 (1H, m, H_{2b}-31), 1.49 (1H, m, H-32), 0.89 (3H, d, $J = 5.1$ Hz, H₃-33), and 0.87 (3H, d, $J = 5.1$ Hz, H₃-33).

Table 1. NMR data for compound **1** in DMSO-*d*₆ (400 and 100 MHz for ¹H and ¹³C, respectively).

position	δ_{C}	δ_{H} , mult. (J in Hz)	COSY	TOCSY	HMBC (H \rightarrow C)
<i>N</i> -Me-l-Phe					
1	167.9				
2	61.3	4.26, dd (11.4, 3.3)	3	3a, 3b	1, 2-NMe, 3, 10
3a	33.9	3.26, dd (14.3, 3.3)	2	2, 3b	2, 4, 5/9
3b		2.78, dd (14.3, 11.5)		2, 3a	2, 4, 5/9
4	137.2				
5/9	128.9	7.09, m	6/8	6/8	3, 6/8, 7
6/8	128.4	7.19, m	5/9, 7	5/9	4, 5/9, 7
7	126.6	7.17, m	5/9		5/9, 6/8
2-NMe	30.4	2.70, s			2, 10
<i>l</i> -Tyr					
10	170.1				
11	49.2	3.99, ddd (8.7, 8.2, 5.3)	11-NH, 12	11-NH, 12	10, 12, 19
12	36.9	a 2.64, dd (14.0, 8.2) b 2.28, dd (14.0, 5.3)	11	11, 11-NH, 12	10, 11, 13, 14/18
13	127.4				
14/18	129.7	6.50, s	15/17	15/17	12, 13, 15/17, 16
15/17	114.6	6.50, s	14/18	14/18	13, 14/18, 16
16	155.3				
11-NH		8.38, d (8.7)	11	11, 12	11, 19
16-OH		9.02, s			15/17
<i>l</i> -Val					
19	169.3				
20	61.0	3.86, t (9.7)	20-NH, 21	20-NH, 21, 22, 23	19, 21, 22, 23, 24
21	30.5	1.66, m	20, 22, 23	20, 20-NH, 22, 23	20, 22, 23
22	19.14	0.78, d (6.6)	21	20, 20-NH, 21, 22	20, 21, 23
23	19.12	0.65, d (6.6)	21	20, 20-NH, 21, 22	20, 21, 22
20-NH		7.00, d (9.7)	20	20, 21, 22, 23	20, 24
<i>l</i> -Pro					
24	170.6				
25	61.0	4.39, dd (8.1, 0.8)	26	26, 27, 28	24, 26, 27, 29
26	31.5	a 2.16, m b 1.99, m	25, 27	25, 26, 27, 28	24, 25, 27, 28
27	21.4	a 1.90, m b 1.66, m	26, 28	25, 26, 27, 28	25, 26, 28
28	46.3	a 3.61, m b 3.38, m	27	25, 26, 27, 28	26, 27
<i>l</i> -Leu					
29	169.3				
30	49.1	4.62, m	30-NH, 31	30-NH, 31, 32, 33, 34,	1, 29, 31
31	41.7	a 1.79, m b 1.29, m	30, 32	30, 30-NH, 31, 32, 33, 34	29, 30, 33, 34
32	24.4	1.49, m	31, 33, 34	30, 30-NH, 31, 33, 34	30, 31, 33, 34
33	22.8	0.89, d (5.1)	32	30, 30-NH, 31, 32, 34	31, 34

position	δ_C	δ_H , mult. (<i>J</i> in Hz)	COSY	TOCSY	HMBC (H \rightarrow C)
34	22.5	0.87, d (5.1)	32	30, 30-NH, 31, 32, 33	31, 33
30-NH		7.05, d (8.4)	30	30, 31, 32, 33, 34	1, 29, 30

The combined 2D NMR data (Fig. 2) and MS/MS analysis (Fig. S14) allowed the identity and connection sequence of the residues. To meet the IHD of 15, **1** must be a cyclic compound; thus, the preliminary structure was established as *cyclo*-(Tyr-*N*-Me-Phe-Leu-Pro-Val). It is worth noting that TOCSY spectrum (Fig. 2C) was particularly helpful to differentiate each spin system in **1**. Furthermore, the MS/MS analysis (Figs. 3 and S14) revealed fragmentation patterns generated from ion fragments m/z 521.2737 $[M - \text{Leu} + \text{H}]^+$ and m/z 471.2950 $[M - \text{Tyr} + \text{H}]^+$, which are in agreement with the proposed structure. Moreover, this fragmentation suggests two main cleavage sites within the peptide (Val/Tyr and Pro/Leu), further confirming the connection of the peptide.

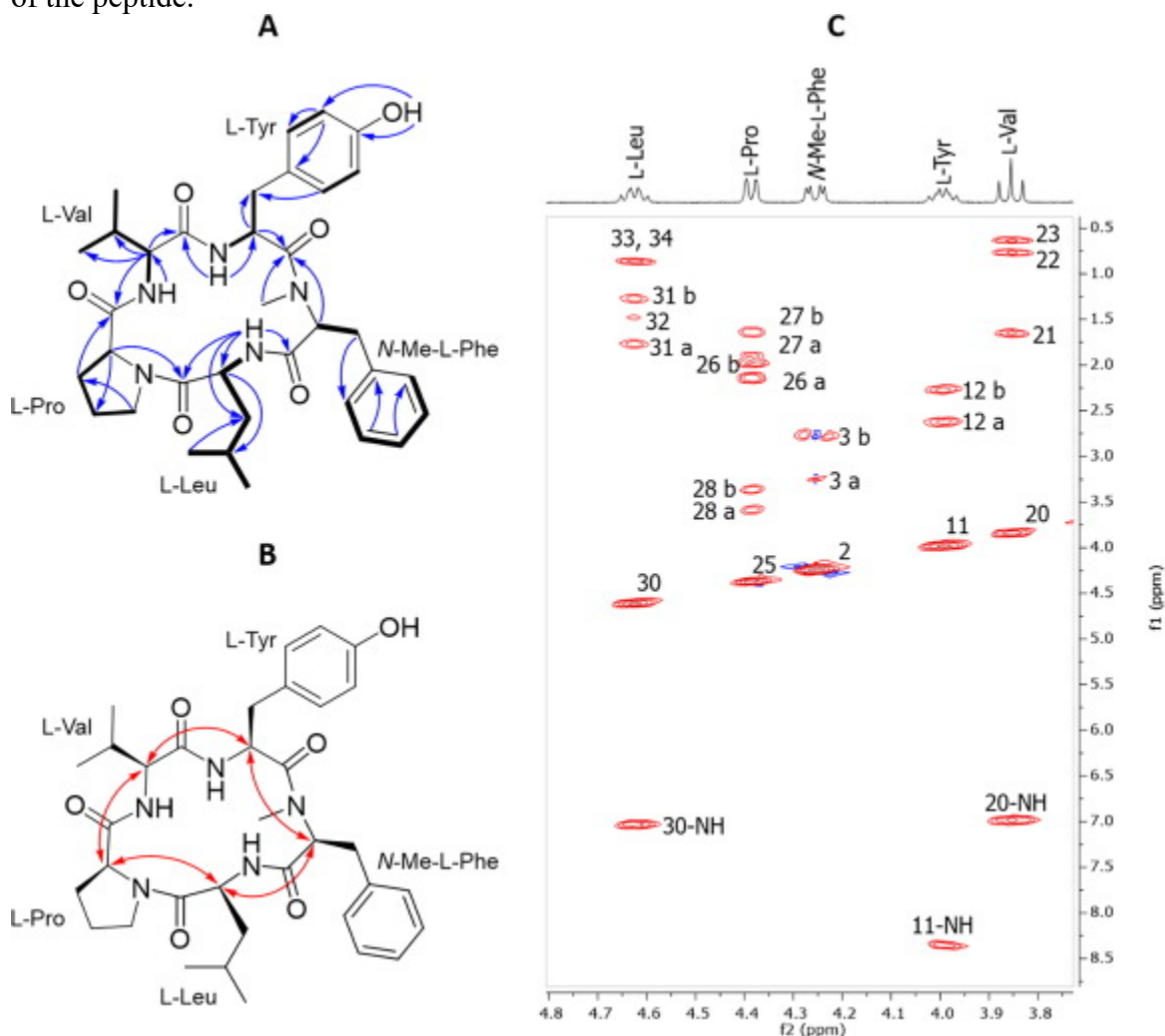


Figure 2. Key (A) COSY (bold lines), HMBC (\rightarrow), and (B) NOESY (\leftrightarrow) correlations observed in **1**. (C) Expansion of t TOCSY spectrum of **1** in DMSO- d_6 (f1 = 0.5–8.5 ppm, f2 = 3.8–4.8 ppm).

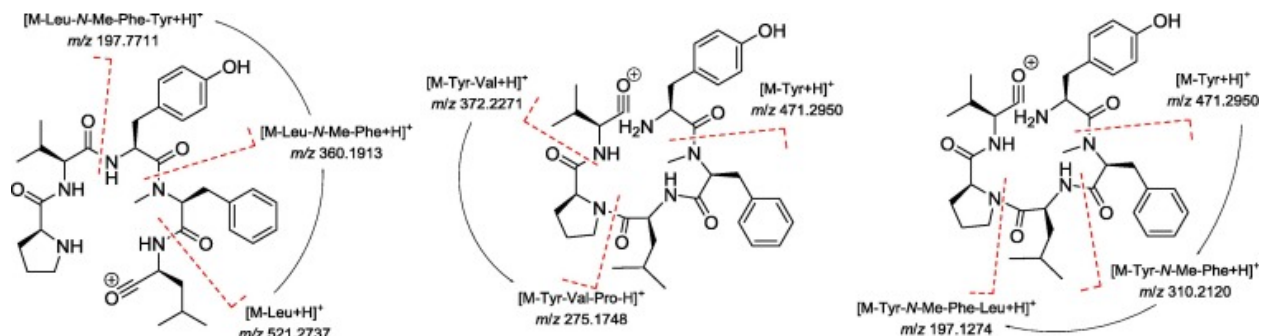


Figure 3. HRESIMS-MS/MS mass fragmentation patterns using Higher-Energy Collisional Dissociation (20 mV) of cyclic peptide **1** showing key amino acid losses.

The relative configuration of **1** was determined with the analysis of the correlations in NOESY spectrum (Figs. 2B and S12); then, a Marfey's analysis was performed to assess the absolute configuration for each residue (Fig. S15) [23], [24]. In this analysis (Fig. S15), it was impossible to achieve full separation of all the amino acids present in the mixture of the derivatized standards under any of the experimental conditions evaluated, particularly between l-Leu and d-Val. To overcome this issue, the HRESIMS data was used: by comparing the mass profiles and mass values for each amino acid, it was possible to confirm the presence of l-Leu in the hydrolysis product of **1** (Fig. S16). This allowed to establish the final structure of **1** as *cyclo*-(l-Tyr-N-Me-l-Phe-l-Leu-l-Pro-l-Val) and was given the trivial name of caletasin.

Compound **2** [25] was obtained as a white amorphous powder and based on the HRESIMS analysis, had a molecular formula of $C_{22}H_{25}O_{10}$ (IHD = 11) (Fig. S8). Its HPLC-UV profile (Fig. S17) was very similar to those of the dibenzopyranones alternariol and alternariol 4-*O*-methyl ether, and its NMR data (Table 2 and Figs. S17–S21) suggested a similar backbone to that of alternariol 4-*O*-methyl ether, with the addition of a 4-*O*-methyl-d-glucopyranose in position 10 [18], [26], [27]. The later was evidenced by a methylated hexose unit corresponding signals in the spectrum: one signal at δ_C 102.0 in the anomeric region [28]; four signals at δ_C 80.8, 78.5, 78.1, 75.4 in the sugar region corresponding to oxygenated carbons; and one signal at δ_C 61.1 corresponding to a methoxy group (Fig. S18) [18], [26], [27]. The site of methylation within the sugar residue was deduced from the HMBC correlation between H-4' (δ_H 3.93, dd, $J = 9.4$, 9.0 Hz) and CH₃O-4' (δ_C 61.1) (Figs. 4 and S19). Additionally, the COSY spectrum provided evidence of the sugar assembly, and the coupling constants of protons H-1' (δ_H 5.70, d, $J = 7.8$ Hz), H-2' (δ_H 4.32, dd, $J = 9.0$, 7.8 Hz), H-3' (δ_H 4.41, t, $J = 9.0$ Hz), and H-4', along with the NOESY between H-1' and H-3', H-3' and H-5', and H-2' and H-4' defined the relative orientation of the hydroxy groups (Figs. 4, S20 and S21). Furthermore, the position of glycosylation was determined by the HMBC correlation between the anomeric proton H-1' and C-10 (δ_C 159.1) of the aglycone portion (Fig. 4). Finally, the D configuration of β -D-4'-methoxyl-glucopyranosyl residue was established by comparison of the specific rotations of aqueous soluble acid hydrolysate product ($\alpha_{D25} + 25$, c 0.08, MeOH) with that of 4-*O*-methyl-d-glucopyranose ($\alpha_{D25} + 80$, c 1.30, MeOH) [29], and the ¹H NMR spectrum of the aglycone, which was identical to that of 4-*O*-methyl-alternariol (Fig. S22) [18], [26].

From all the isolated compounds, only alternariol and beauvericin showed antimicrobial activity against *B. subtilis* (MIC = 40 and 2.5 μ g/mL, respectively; positive control, vancomycin, MIC = 10 μ g/mL) and *S. aureus* (MIC = 20 and 10 μ g/mL, respectively; positive control,

ampicillin, MIC = 1.25 $\mu\text{g/mL}$) (Supplementary data). Additionally, compounds **1** and **2** were inactive (IC₅₀ less than 25 μM) when tested against MDA-MB-435, MDA-MB-231, and OVCAR3 cells lines (Table S2). Finally, none of the tested compounds exhibited inhibitory activity against seed germination and radicle growth of *Amaranthus hypochondriacus* (Supplementary data).

Table 2. NMR for compound **2** in pyridine-*d*₅ (500 and 125 for ¹H and ¹³C, respectively).

position	δ_{C} , type		δ_{H} , mult. (<i>J</i> in Hz)
1	100.3	C	
2	166.0	C	
3	100.4	CH	6.82, d (2.2)
4	167.2	C	
5	105.3	CH	7.29, d (2.2)
6	139.2	C	
7	112.6	C	
8	138.5	C	
9	119.1	CH	7.07, d (2.6)
10	159.1	C	
11	103.8	CH	7.25, d (2.7)
12	153.7	C	
13	166.0	C	
1'	102.0	CH	5.70, d (7.8)
2'	75.4	CH	4.32, dd (9.0, 7.8)
3'	78.5	CH	4.41, t (9.0)
4'	80.8	CH	3.93, dd (9.4, 9.0)
5'	78.1	CH	4.02, m
6'	62.1	CH ₂	4.36, dd (12.3, 2.0) 4.24, dd (12.3, 4.7)
CH ₃ O-4	56.2	CH ₃	3.81, s
CH ₃ O-4'	61.1	CH ₃	3.90, s
CH ₃ -8	25.8	CH ₃	2.66, s

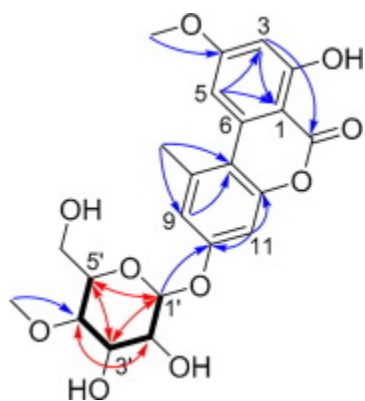


Figure 4. Key COSY (bold lines), HMBC (→) and NOESY (↔) correlations observed in **2**.

Acknowledgments

We thank Tyler Graf, Daniel Todd, and Franklin Moy from UNCG, for their assistance in the chromatographic, HRMS and NMR techniques, respectively. The HRMS data were acquired in the Triad Mass Spectrometry Laboratory at the UNCG. This work was supported by grants from CONACyT-CB 236564, CONACyT-INFRA 252226, UNAM-DGAPA IA205017, and FQ-PAIP

5000-9145. This bioassay and fungal ID data were generated with partial support via grant P01 CA125066 from the National Cancer Institute/National Institutes of Health, Bethesda, MD, USA. M.A.A.-C. acknowledges a fellowship from CONACyT (274048) to pursue graduate studies, and thanks the Posgrado en Ciencias Químicas and the Programa de Movilidad Internacional, UNAM, for their financial support during his stay at UNCG. M.F. thanks Rachel Mata for being a guide and an inspiration in the study of Mexican natural products.

Appendix A. Supplementary data

Supplementary data to this article can be found online at <https://doi.org/10.1016/j.tetlet.2019.05.037>.

References

- [1] D.L. Hawksworth, R. Lucking, *Microbiol. Spectrum* 5 (2017) FUNK-0052-2016.
- [2] E. Aguirre-Acosta, M. Ulloa, S. Aguilar, J. Cifuentes, R. Valenzuela, *Rev. Mex. Biodivers.* 85 (2014) S76–S81.
- [3] R. Mata, M. Figueroa, I. Rivero-Cruz, M.L. Macias-Rubalcava, *Planta Med.* 84 (2018) 594–605.
- [4] M.A. Aparicio-Cuevas, I. Rivero-Cruz, M. Sanchez-Castellanos, D. Menendez, H. A. Raja, et al., *J. Nat. Prod.* 80 (2017) 2311–2318.
- [5] T. Amagata, M. Doi, M. Tohgo, K. Minoura, A. Numata, *Chem. Commun.* (1999) 1321–1322.
- [6] T. Amagata, K. Minoura, A. Numata, *J. Nat. Prod.* 69 (2006) 1384–1388.
- [7] T. Amagata, M. Tanaka, T. Yamada, K. Minoura, A. Numata, *J. Nat. Prod.* 71 (2008) 340–345.
- [8] T. Amagata, M. Tanaka, T. Yamada, Y.-P. Chen, K. Minoura, et al., *Tetrahedron Lett.* 54 (2013) 5960–5962.
- [9] B. Clark, R.J. Capon, E. Lacey, S. Tennant, J.H. Gill, et al., *J. Nat. Prod.* 68 (2005) 1226–1230.
- [10] B.R. Clark, R.J. Capon, E. Lacey, S. Tennant, J.H. Gill, *Org. Lett.* 8 (2006) 701–704.
- [11] L. Hammerschmidt, A.H. Aly, M. Abdel-Aziz, W.E. Muller, W. Lin, et al., *Bioorg. Med. Chem.* 23 (2015) 712–719.
- [12] S. Kitchawalit, K. Kanokmedhakul, S. Kanokmedhakul, K. Soyong, *Nat. Prod. Res.* 28 (2014) 1045–1051.

- [13] T. Suga, T. Ishii, M. Iwatsuki, T. Yamamoto, K. Nonaka, et al., *J. Antibiot.* 65 (2012) 527–529.
- [14] H. Wang, H. Dai, C. Heering, C. Janiak, W. Lin, et al., *RSC Adv.* 6 (2016) 81685–81693.
- [15] T. Liu, S.L.F. Meyer, D.J. Chitwood, K.R. Chauhan, D. Dong, et al., *J. Agric. Food Chem.* 65 (2017) 3127–3132.
- [16] K.V. Rao, A.K. Sadhukhan, M. Veerender, V. Ravikumar, E.V. Mohan, et al., *Chem. Pharm. Bull.* 48 (2000) 559–562.
- [17] N. Kushida, T. Yaguchi, N. Miike, Japan Patent 2001288005, 2003.
- [18] G.-B. Xu, X. Pu, H.-H. Bai, X.-Z. Chen, G.-Y. Li, *Nat. Prod. Res.* 29 (2015) 848–852.
- [19] K. Koch, J. Podlech, E. Pfeiffer, M. Metzler, *J. Org. Chem.* 70 (2005) 3275–3276.
- [20] R.L. Hamill, C. Higgins, H. Boaz, M. Gorman, *Tetrahedron Lett.* 10 (1969) 4255–4258.
- [21] Caletasin (1): orange powder; $[\alpha]_{23}^D -684$ (c 0.1, CHCl₃); UV (MeOH) k_{max} (log e) 277 (2.53), 237 (2.53); ¹H and ¹³C NMR, see Table 1; HRESIMS m/z 634.3596 [M + H]⁺ (calcd. for C₃₅H₄₈N₅O₆ 634.3526).
- [22] L.J. Fremlin, A.M. Piggott, E. Lacey, R.J. Capon, *J. Nat. Prod.* 72 (2009) 666–670.
- [23] S. Ayers, B.M. Ehrmann, A.F. Adcock, D.J. Kroll, E.J. Carcache de Blanco, et al., *J. Pept. Sci.* 18 (2012) 500–510.
- [24] M. Figueroa, H. Raja, J.O. Falkinham 3rd, A.F. Adcock, D.J. Kroll, et al., *J. Nat. Prod.* 76 (2013) 1007–1015.
- [25] 4-O-methylalternariol-10-O-β-D-(4-methoxyl-glucopyranoside) (2): white amorphous powder; $[\alpha]_{20}^D +25$ (c 0.08, MeOH); UV (DMSO) k_{max} (log e) 339 (2.35), 300 (2.29), 289 (2.29); ¹H and ¹³C NMR, see Table 2; HRESIMS m/z 449.1440 [M + H]⁺ (calcd. for C₂₂H₂₅O₁₀ 449.1442).
- [26] A.A. Hildebrand, B.N. Kohn, E. Pfeiffer, D. Wefers, M. Metzler, et al., *J. Agric. Food Chem.* 63 (2015) 4728–4736.
- [27] S.T. Soukup, B.N. Kohn, E. Pfeiffer, R. Geisen, M. Metzler, et al., *J. Agric. Food Chem.* 64 (2016) 8892–8901.
- [28] R. Pereda-Miranda, D. Rosas-Ramírez, J. Castañeda-Gómez, in: *Fortschritte der Chemie organischer Naturstoffe / Progress in the Chemistry of Organic Natural Products*. Springer Wien New York, Vienna, 2010; Vol. 92. pp. 77–153.

[29] S. Saepua, J. Kornsakulkarn, W. Somyong, P. Laksanacharoen, M. Isaka, et al., *Tetrahedron* 74 (2018) 859–866.